Dissecting Myocardial Mechanics in Patients With Severe Aortic Stenosis: 2-Dimensional vs 3-Dimensional–Speckle Tracking Echocardiography

Xiaojun Bi
Mayo Clinic Minnesota
Husam M. Salah
Jordan University of Science and Technology
Maria C. Arciniegas Calle
Mayo Clinic Minnesota
Jeremy J. Thaden
Mayo Clinic Minnesota
Lara F. Nhola
Mayo Clinic Minnesota
Hartzell V. Schaff
Mayo Clinic Minnesota
Sorin V. Pislaru
Mayo Clinic Minnesota
Patricia A. Pellikka
Mayo Clinic Minnesota
Alberto Pochettino
Mayo Clinic Minnesota
Kevin L. Greason
Mayo Clinic Minnesota
Vuyisile T. Nkomo
Mayo Clinic Minnesota
Hector R. Villarraga (villarraga.hector@mayo.edu)
Mayo Clinic Minnesota https://orcid.org/0000-0002-3675-6948

Research article

Keywords: aortic stenosis; echocardiography; stage B heart failure; strain; 3 dimensional–speckle-tracking echocardiography; valvulo-arterial impedance

Posted Date: September 10th, 2019

DOI: https://doi.org/10.21203/rs.2.14188/v1

Version of Record: A version of this preprint was published at BMC Cardiovascular Disorders on January 30th, 2020. See the published version at https://doi.org/10.1186/s12872-020-01336-0.

Abstract

Background: Aortic valve stenosis (AS) commonly causes left ventricular (LV) pressure overload; thus, identifying patients with adverse remodeling/early LV dysfunction is critical. We compared 2-dimensional (2D) to 3-dimensional (3D) echocardiographic measures of LV myocardial deformation in patients with severe AS and studied the relation of LV preload and afterload (Zva) to myocardial deformation. Methods: We prospectively included 168 symptomatic patients (72±12 years) with severe AS and ejection fractions ≥50%. Strain parameters from those patients were compared with normal values found in the literature. 3D full-volume and 2D images were analyzed for global longitudinal strain (GLS), global radial strain (GRS), global circumferential strain (GCS), systolic strain rate (SRs), basal rotation (Rotmax-B), apical rotation (Rotmax-A), and peak systolic twist (Twistmax). Results: 2D–GLS and 2D–GCS decreased significantly compared with normal values (P□.001 and P=.02, respectively); 2D Rotmax-B and Twistmax increased (P□.001 vs normal values). Agreement between 2D–GLS and 3D–GLS by concordance correlation coefficient was 0.49 (95% CI, 0.39-0.57) in patients with AS. Both 2D– and 3D–GLS correlated with valvulo-arterial impedance (Zva) (r=0.34, P<.001; and r=0.23, P=.003, respectively). Conclusion: In patients with severe AS, GLS and GCS decreased, and basal rotation and twist increased to maintain LV ejection fraction. 2D– and 3D–GLS had a relatively fair agreement. Both 2D– and 3D–GLS correlated modestly with Zva.

Background

Aortic valve stenosis (AS), which is the most common native valve disease, is characterized by left ventricular (LV) pressure overload. In patients with AS, the left ventricle often faces 2 afterloads: valvular and arterial (1,2). The increasing afterload can lead to LV remodeling and a change in coronary flow reserve. These alterations can cause subendocardial ischemia and fibrosis and may gradually affect LV systolic function (3-5). LV ejection fraction (LVEF) is the most important conventional parameter used to assess LV myocardial function. However, it is well known that LVEF is an index reflecting LV chamber function. A decrease in LVEF usually occurs at an end stage of severe AS (6, 7). Global longitudinal strain by 2-dimensional (2D) echocardiography can be used to detect early systolic dysfunction and has been proposed as an important marker of LV function in patients with AS (8-11). However, the process of ventricular contraction is very complex because relaxation occurs in 3 dimensions and cannot be comprehensively quantified by 2D echocardiography (12,13). For this reason, 3-dimensional (3D) echocardiography and speckle tracking strain imaging are promising techniques that may provide a more complete picture of myocardial deformation (14,15). New insights into LV remodeling and myocardial deformation could potentially improve our ability to identify patients at high risk for adverse remodeling or early LV dysfunction. Currently published studies are small and provide only limited and conflicting data on how myocardial deformation is affected by aortic stenosis, as measured by 3D–speckle-tracking echocardiography (3D–STE) (3,4,16,17). Therefore, the purpose of this prospective study was 1) to determine whether and how myocardial deformation in 2D and 3D is affected in patients with severe AS and normal LVEF vs normal values found in the literature; 2) to compare 2D to 3D echocardiographic

measures of LV myocardial deformation in patients with severe AS; and 3) to characterize the relationship of LV preload, afterload, and valvulo-arterial impedance (Z_{va}) with myocardial deformation, as measured by 2D and 3D echocardiography.

Methods

Study Population

We prospectively recruited 178 symptomatic patients who had been evaluated for severe AS, defined as a mean gradient of at least 40 mm Hg or an aortic valve area less than 1.0 cm^2, and who had a normal ejection fraction (EF), defined as greater than 50%, on conventional transthoracic echocardiography (TTE). The study was performed at Mayo Clinic, Rochester, Minnesota, from November 1, 2014, through August 31, 2015. Patients were excluded if they had moderate or greater aortic regurgitation, moderate or greater mitral regurgitation, an irregular R-R interval, and were less than 18 years old, or if image quality was inadequate. The final analysis included 168 patients. All patients underwent additional conventional echocardiography and real-time 3D echocardiography. Vital signs were measured in all patients immediately before the echocardiographic examination. Demographic and clinical characteristics of the study population are presented in Table 1. This study was approved by the Mayo Clinic Institutional Review Board, and all patients gave informed consent to participate.

Image Acquisition and Analysis

Each patient underwent a standard 2D–TTE and a real-time 3D echocardiogram in the left lateral decubitus position, using commercially available equipment (IE33 and EPIQ7, Philips Medical Systems, Andover, Massachusetts) with a fully sampled matrix-array transducer (X5-1). Studies were performed by an experienced cardiologist (X.B.). 3D full volume was acquired from the apical window with a high-volume rate (average, ≥30 volumes/s) and 6-beat acquisition, allowing for full coverage of the entire left ventricle by the pyramidal volume. Patients were told to hold their breath during image acquisition. Images were optimized for endocardial border visualization before acquisitions; overall gain was modified and time gain and compression adjusted, as needed. The acquired 2D images and 3D full-volume images were analyzed offline with TomTec 4D Echo software, version 4.6 (TomTec Imaging Systems, Image Arena, Unterschleissheim, Germany).

For 2D echocardiography, the standard 2D, M-mode, and Doppler measurements were obtained in accordance with guidelines from the American Society of Echocardiography. LV end-diastolic volume (LVEDV), end-systolic volume (LVESV), and ejection fraction (LVEF) were measured manually by using the biplane Simpson method. Three standard apical views (4-chamber, long-axis, and 2-chamber) were obtained for the assessment of global longitudinal strain (GLS) and global longitudinal systolic strain rate (GLSR), and 3 parasternal short-axis views (basal, mid, and apical levels) were obtained for the assessment of global radial strain (GRS) and global radial systolic strain rate (GRSR), global

circumferential strain (GCS) and global circumferential systolic strain rate (GCSR), and LV apical peak systolic rotation (Rot_{max}-A), LV basal peak systolic rotation (Rot_{max}-B), and peak systolic twist ($Twist_{max}$).

For 3D echocardiography, 3 standard apical views were automatically extracted from the 3D full-volume data sets. The mitral annulus and the LV apex were manually selected as the landmarks to initialize the LV boundaries. Then, the 3D endocardial surface was automatically reconstructed at end diastole and end systole. The endocardial surface reconstruction was manually adjusted, as necessary, and the papillary muscles were included as part of the LV cavity. Subsequently, 3D–speckle tracking was automatically characterized. The software provided anatomical longitudinal, radial, circumferential, and principal tangential strain/time curves for the 16 segments and peak global strain, as well as averaged peak strain at 3 LV levels (basal, mid-ventricular, and apical) (Figure 1).

To measure afterload, total arterial stiffness (TAS) was measured by the formula: TAS = pulse pressure/stroke volume (SV); total arterial compliance (TAC) was measured by the formula: TAC = SV/pulse pressure; effective arterial elastance (EAE) was measured by the formula: EAE = end systolic pressure/SV; systemic vascular resistance (SVR) was measured by the formula: SVR = [80 × (mean arterial pressure - right atrial pressure)]/cardiac output; systemic vascular resistance index (SVRI) was measured by the formula: SVRI = [80 × (mean arterial pressure - right atrial pressure)]/cardiac index (18). Briand et al (1) proposed a simple index to measure global LV afterload called the Z_{va}, which can be calculated by the formula: $Z_{va} = (SAP + MG_{net})/SVI$, where SAP is the systolic arterial pressure, MG_{net} is the mean net pressure gradient transvalvular pressure, and SVI is the stroke volume index. Therefore, Z_{va} represents the valvular and arterial factors that oppose ventricular systole by absorbing the mechanical energy developed by the left ventricle (19).

Intraobserver and Interobserver Variability of 2D– and 3D–Speckle Tracking Measurements

For reproducibility of 2D– and 3D–speckle-tracking echocardiographic measurements of deformation parameters, 20 patients were randomly selected and reanalyzed by the same observer to determine the intraobserver agreement and by a second experienced echocardiographer, who was blinded to the initial results, to determine the interobserver agreement. Both measurements were obtained with the intraclass correlation coefficient (ICC).

Statistical Analysis

Data were presented as the mean±SD for continuous variables and as percentages for categorical variables. Agreement between parameters in 2D and 3D were assessed using the concordance correlation coefficient (CCC) with 95% CI. Associations between 2 continuous variables were measured using the Pearson or Spearmen correlation (P) coefficient. Variability between the 2 sets of measurements was reported as the mean difference ±SD and the ICC with 95% CI. Means were compared using a *z* test or *t* test when no SD was available for the normal-value data. Data were analyzed with JMP 10.0 software (SAS Institute Inc, Cary, North Carolina) and MedCalc statistical software, version 11.4.1.0 (MedCalc

Software, Ostend, Belgium). All probability values were 2-sided, and a *P* value <.05 was considered statistically significant.

Results

Parameters of 2D and 3D Echocardiography

2D and 3D echocardiographic parameters are shown in Table 2. Data from patients with AS was compared with normal values found in the literature.

Wall thickness and LV mass were greater in the study patients compared with normal values (*P*<.001). The mitral inflow, tissue velocity, and early mitral inflow velocity/early diastolic mitral annular tissue velocity (E/e') ratio were significantly different between cases and normal values (P<.001). The LVEDV, LV end-diastolic diameter (LVEDD), interventricular septal thickness in diastole (IVSD), LV posterior wall diameter (LVPWD), LVESV, and the SV on 2D echocardiography, were significantly different between the 2 groups (*P*<.0001). When we focused on the differences between 2D and 3D in the AS study patients, only LVEF was significantly lower when measured by 3D (*P*<.001); however, it remained within normal clinical limits. The calculated indexes of LV afterload in the study patients with AS were as follows: total arterial stiffness, 0.8±0.3 mm Hg/mL; total arterial compliance, 1.5±0.7 mL/mm Hg; systemic vascular resistance, 1368±438 mL/mm Hg/m^2; systemic vascular resistance index, 2628±788 dynes × s/cm^{-5}; and Z_{va}, 3.7±0.7 mm Hg/mL/m^2.

Parameters of Speckle-Tracking Strain Imaging in 2D and 3D

The parameters of 2D– and 3D–speckle-tracking strain for both groups are shown in Table 3. For the 2D images, GLS and GCS were significantly lower for patients than the normal values (*P*<.001). Rot_{max}-A, Rot_{max}-B, and $Twist_{max}$ were significantly different in patients with AS vs the normal values (*P*<.001). The mean GLSRs, 1/s, was measured as 1.0±0.1, GRSRs 1/s as 2.0±0.4, and GRSRs, 1/s, as –1.8±0.4.

Comparison of 3D Imaging With 2D Echocardiographic Data

The agreement of echocardiographic data between 3D and 2D images is shown in Figures 2 and 3. A relatively fair level of agreement existed between 2D–GLS and 3D–GLS (CCC=0.49; 95% CI, 0.39 to 0.57 and ρ, 0.54 [*P*<.0001]) for patients with severe AS. The agreement between 3D and 2D images was poor for GCS (CCC=0.29; 95% CI, 0.16 to 0.41 and ρ, 0.23 [*P*<.002]), and GRS (CCC=0.10; 95% CI, -0.04 to 0.23 and ρ, –0.2 [*P*<.02], and $Twist_{max}$ (CCC=0.11; 95% CI, 0 to 0.21). An excellent level of agreement existed between 3D–LVEDV and 2D–LVEDV (CCC=0.89; 95% CI, 0.85 to 0.91) (Figure 3). A fair level of agreement existed between 2D–LVEF and 3D–LVEF (CCC=0.51; 95% CI, 0.39 to 0.61).

Relation Between Parameters of LV Speckle-Tracking Strain in 2D and 3D Imaging With Preload and Afterload

Both 2D– and 3D–GLS correlated with Z_{va} (r=0.34, *P*.001; r=0.23, *P*=.003, respectively). The other deformation parameters, including Rot_{max}-A and $Twist_{max}$ in 2D and 3D, did not correlate with Z_{va}. Among all the indexes of afterload, only Z_{va} correlated modestly with 2D–GLS and 3D–GLS; the other indexes had no correlation. The LVEDV index correlated less but was still statistically significant (2D–GLS, r=0.14; *P*=.04; 3D–GLS, r=0.22; *P*<.001).

Intraobserver and Interobserver Variability

Table 4 shows the results of the intraobserver and interobserver variability for 2D–STE (2D–speckle-tracking echocardiography) and 3D–STE measurements. Our results showed excellent correlation, with values ranging from 0.84 to 0.95 and a mean of 0.90.

Discussion

The main finding from this study was an increased basal rotation (Rot_{max}-B) as well as twist ($Twist_{max}$) that compensates for the reduction in LV longitudinal and circumferential deformation in patients with severe AS, thus allowing the ventricle to maintain LVEF. The counter-coiled helix, which is composed of subepicardial and subendocardial fibers, generates an LV twist that has been proven to be fundamental to LV systole and, therefore, EF (22,23). The direction of LV twist is governed by the larger radial fibers at the subepicardium. Several previous studies have reported good correlation between LV twist derived from 2D–speckle-tracking echocardiography and magnetic resonance imaging (24,25). In our study, Rot_{max}-B and $Twist_{max}$ in 2D images dramatically increased, a finding consistent with other reports (21,26). Possibly, subendocardial ischemia leads to a reduction of the opposing rotational forces of the subendocardial fibers, which would increase the difference in radius between the subepicardium and subendocardium. Such alterations would increase the arm of movement governed by the fibers of the subepicardium. In addition, LV hypertrophy might increase the arm force. More importantly, increased rotation and $Twist_{max}$ may be compensating for the reduction of LV deformation in the other directions in patients with AS (26). All of these potential mechanisms may theoretically also lead to increased Rot_{max}-B.

Furthermore, twist was also significantly increased in AS study patients compared with normal values. Our results confirm that LV twist has an important role in LV ejection, which could explain why LVEF and cardiac output are preserved in patients with severe AS, but LV systolic function is impaired. A recent study by Musa et al (27) showed that transcatheter aortic valve implantation and surgical aortic valve replacement procedures were associated with comparable declines in rotational LV mechanics.

It is widely acknowledged that myocardial deformation on echocardiography can be described by 3 directions: longitudinal (LS), circumferential (CS), and radial (RS). LS denotes contraction of the longitudinally arranged endocardial fibers; CS denotes contraction of the circumferentially arranged mid-layer fibers; RS is defined as contraction of all the wall thickness (8,28). In patients with severe AS, the increasing afterload may lead to hypertrophy, decreased coronary perfusion, myocardial ischemia, and

fibrosis. The endocardium is usually the most vulnerable to increased wall stress and stress-induced ischemia with LV pressure overload (29). As a result, impairment of GLS usually occurs first among other strains.

The finding of decreased GLS in 2D and 3D is consistent with other reports (4,5,30). We also found that GCS on 3D echocardiography was not significantly different when compared with 2D measurements (3). In our study, 2D echocardiography–derived GCS decreased significantly, and GRS had no significant change. Delgado et al (17) observed a significant decrease in all strain directions in 2D images. This variability in studies may be due to differences in patient populations, as well as differences in software. The cohorts in the Li et al (3) and Delgado et al (17) studies were also younger, and the sample sizes were smaller. Moreover, GRS does not represent a specific set of muscle fibers, and the variation for this parameter is always greater (31). Our results confirm that GLS is consistently impaired when compared with other parameters of deformation and is compensated by an increase in twist.

In patients with degenerative AS, arterial compliance is frequently reduced, which contributes to increased afterload and decreased LV function. Hence, the left ventricle is often subjected to a double afterload—from valvular obstruction and from the systemic arterial system (1,2,18,32). Z_{va}, a simple index proposed by Briand et al (1), provides an estimate of the global hemodynamic load imposed on the left ventricle and is an important index of AS severity and a predictor of LV dysfunction. We found that Z_{va} was moderately elevated in patients with severe AS (33). A study by Pagel et al (34) showed that aortic valve replacement affected only the valvular component of afterload and had no effect on arterial compliance in elderly patients, which suggests that other comorbidities, such as hypertension and atherosclerosis, may have an important impact on this parameter.

Our study showed a correlation between 2D– and 3D–GLS and Z_{va} but no significant relationship between Z_{va} and other deformation parameters (GRS, GCS). We also found that impaired GLS, both in 2D and 3D, correlated with increasing LVEDV and E/e¢ ratio. Sato et al (35) had similar findings; diastolic dysfunction was present in their patients, although their study patients had low-flow, low-gradient severe AS. The increase in Z_{va}, combined with the increased LVEDV, reflected a large global hemodynamic overload. According to the Laplace law, patients with severe AS are likely to have markedly increased wall stress, which may lead to depressed myocardial contractility. Maréchaux et al (19) reported similar results, confirming that LV longitudinal contraction is, in large part, determined by LV preload and afterload.

Previous studies have reported conflicting results of comparisons of 2D– and 3D–STE measurements, possibly because of major differences in the study populations (sample sizes and the severity of AS) and methodology (ie, software) (3,15,36,37). In a study by Altman et al (16), 3D–STE was not shown to be superior to 2D–STE for any of the 3 components of LV deformation. In our study, we found a modest agreement between 2D–GLS and 3D–GLS assessed with CCC; agreement of other 2D and 3D strain parameters was poor. We also observed a similar correlation between 2D– and 3D–GLS and Z_{va}. Theoretically, 3D–STE should be more accurate than 2D–STE because 3D–STE can overcome

well-known limitations of 2D–STE: 3D images can avoid foreshortening of apical views, and 3D images are able to give a more complete picture of myocardial deformation in 3 dimensions and, therefore, eliminate, to an extent, the problem of out-of-plane motion, which may affect the accuracy of LV strain and twist measurements with 2D echocardiography. However, the lower temporal and spatial resolutions of 3D images are potential limitations and could adversely affect the accuracy of 3D–STE measurements in patients with 3D images at the lower frame rates (36,37).

Conclusions

In patients with severe AS, GLS is consistently compromised, and LVEF and cardiac output are maintained by increased basal rotation and twist. 3D–STE is comparable to 2D–STE. 2D–GLS correlated modestly with Z_{va}. No significant correlation between Z_{va} and other deformation parameters (i.e., GRS, and GCS) was observed.

Limitations

This was a single-center, single-ethnicity, observational study. We also did not validate deformation measurements against reference standards, including tagged magnetic resonance imaging or sonomicrometry. The relatively low frame rate of real-time 3D echocardiographic imaging could potentially lead to underestimating strain values. In addition, the relatively high body mass index in our cohort may have led to poor image quality. It is widely acknowledged that the accuracy of both 3D– and 2D–STE depends on image quality. Finally, the various software vendors used different analysis algorithms, including for the image format, numeric filters, and interpolation techniques, all of which affected the measurements. Finally, our results cannot be extrapolated to other ultrasound machine systems or 3D–speckle tracking software.

Abbreviations

2D, 2-dimensional

3D, 3-dimensional

2D–STE, 2D–speckle-tracking echocardiography

3D–STE, 3D–speckle-tracking echocardiography

AS, aortic valve stenosis

CCC, concordance correlation coefficient

CS, circumferential strain

E/e', ratio of the early wave of mitral inflow and early diastolic tissue Doppler velocity at the septal mitral annulus

EAE, effective arterial elastance

EF, ejection fraction

GCS, global circumferential strain

GCSR, global circumferential strain rate

GLS, global longitudinal strain

GLSR, global longitudinal strain rate

GRS, global radial strain

GRSR, global radial strain rate

ICC, intraclass correlation coefficient

IVSD, interventricular septum in diastole[Q]

LS, longitudinal strain

LV, left ventricular

LVEDD, left ventricular end-diastolic diameter

LVEDV, left ventricular end-diastolic volume

LVEF, left ventricular ejection fraction

LVESV, left ventricular end-systolic volume

LVPWD, left ventricular posterior wall diameter

MGnet, mean net pressure gradient

P, Spearmen correlation

Rot_{max}-A, left ventricular apical peak systolic rotation

Rot_{max}-B, left ventricular basal peak systolic rotation

RS, radial strain

SAP, systolic arterial pressure

SV, stroke volume

SVI, stroke volume index

SVR, systemic vascular resistance

SVRI, systemic vascular resistance index

TAC, total arterial compliance

TAS, total arterial stiffness

TTE, transthoracic echocardiography

$Twist_{max}$, peak systolic twist

Z_{va}, valvulo-arterial impedance

Declarations

Ethics approval and consent to participate

This study was approved by the Mayo Clinic Institutional Review Board, and all patients gave informed consent to participate. All patients gave written consent.

Consent for publication

not applicable.

Availability of data and materials

The datasets generated and/or analyzed during the current study are not publicly available because the information and data of the study population were extracted from Hospital Information System and were recorded manually in EXCEL to form our private database. But the data are available from the corresponding author on reasonable request.

Competing interests

The authors of this article have no competing interest.

Fundings

This research did not receive any grants from funding agencies in the public, commercial, or not-for-profit sectors.

Author's contributions

Conception and design of the study: XB, VTN, HRV

Acquisition of data or analysis and interpretation of data: JJT, LFN, KLG, AP, HVS

Drafting the article or revising it critically for important intellectual content: HRV, XB, MCC, SVP, PAP, HMS

All authors gave final approval of the version to be submitted.

References

1. Briand M, Dumesnil JG, Kadem L, Tongue AG, Rieu R, Garcia D, et al. Reduced systemic arterial compliance impacts significantly on left ventricular afterload and function in aortic stenosis: implications for diagnosis and treatment. J Am Coll Cardiol. 2005 Jul 19;46(2):291-8.
2. Garcia D, Barenbrug PJ, Pibarot P, Dekker AL, van der Veen FH, Maessen JG, et al. A ventricular-vascular coupling model in presence of aortic stenosis. Am J Physiol Heart Circ Physiol. 2005 Apr;288(4):H1874-84. Epub 2004 Dec 16.
3. Li CM, Li C, Bai WJ, Zhang XL, Tang H, Qing Z, et al. Value of three-dimensional speckle-tracking in detecting left ventricular dysfunction in patients with aortic valvular diseases. J Am Soc Echocardiogr. 2013 Nov;26(11):1245-52. Epub 2013 Aug 28.
4. Dusenbery SM, Lunze FI, Jerosch-Herold M, Geva T, Newburger JW, Colan SD, et al. Left ventricular strain and myocardial fibrosis in congenital aortic stenosis. Am J Cardiol. 2015 Oct 15;116(8):1257-62. Epub 2015 Jul 28.
5. Eidet J, Dahle G, Bugge JF, Bendz B, Rein KA, Aaberge L, et al. Intraoperative improvement in left ventricular peak systolic velocity predicts better short-term outcome after transcatheter aortic valve implantation. Interact Cardiovasc Thorac Surg. 2016 Jan;22(1):5-12. Epub 2015 Oct 13.
6. Weidemann F, Herrmann S, Stork S, Niemann M, Frantz S, Lange V, et al. Impact of myocardial fibrosis in patients with symptomatic severe aortic stenosis. Circulation. 2009 Aug 18;120(7):577-84. Epub 2009 Aug 3.
7. Miyazaki S, Daimon M, Miyazaki T, Onishi Y, Koiso Y, Nishizaki Y, et al. Global longitudinal strain in relation to the severity of aortic stenosis: a two-dimensional speckle-tracking study. Echocardiography. 2011 Aug;28(7):703-8. Epub 2011 May 12.
8. Deng YB, Liu R, Wu YH, Xiong L, Liu YN. Evaluation of short-axis and long-axis myocardial function with two-dimensional strain echocardiography in patients with different degrees of coronary artery stenosis. Ultrasound Med Biol. 2010 Feb;36(2):227-33. Epub 2010 Jan 4.

9. Fine NM, Shah AA, Han IY, Yu Y, Hsiao JF, Koshino Y, et al. Left and right ventricular strain and strain rate measurement in normal adults using velocity vector imaging: an assessment of reference values and intersystem agreement. Int J Cardiovasc Imaging. 2013 Mar;29(3):571-80. Epub 2012 Sep 14.
10. Bi X, Deng Y, Zeng F, Zhu Y, Wu Y, Zhao C, et al. Evaluation of epirubicin-induced cardiotoxicity by two-dimensional strain echocardiography in breast cancer patients. J Huazhong Univ Sci Technolog Med Sci. 2009 Jun;29(3):391-4. Epub 2009 Jun 10.
11. Ng AC, Delgado V, Bertini M, Antoni ML, van Bommel RJ, van Rijnsoever EP, et al. Alterations in multidirectional myocardial functions in patients with aortic stenosis and preserved ejection fraction: a two-dimensional speckle tracking analysis. Eur Heart J. 2011 Jun;32(12):1542-50. Epub 2011 Mar 29.
12. Maffessanti F, Nesser HJ, Weinert L, Steringer-Mascherbauer R, Niel J, Gorissen W, et al. Quantitative evaluation of regional left ventricular function using three-dimensional speckle tracking echocardiography in patients with and without heart disease. Am J Cardiol. 2009 Dec 15;104(12):1755-62.
13. Muraru D, Cucchini U, Mihaila S, Miglioranza MH, Aruta P, Cavalli G, et al. Left ventricular myocardial strain by three-dimensional speckle-tracking echocardiography in healthy subjects: reference values and analysis of their physiologic and technical determinants. J Am Soc Echocardiogr. 2014 Aug;27(8):858-871.e1. Epub 2014 Jun 26.
14. Saito K, Okura H, Watanabe N, Hayashida A, Obase K, Imai K, et al. Comprehensive evaluation of left ventricular strain using speckle tracking echocardiography in normal adults: comparison of three-dimensional and two-dimensional approaches. J Am Soc Echocardiogr. 2009 Sep;22(9):1025-30. Epub 2009 Jun 24.
15. Stefani L, De Luca A, Toncelli L, Pedrizzetti G, Galanti G. 3D Strain helps relating LV function to LV and structure in athletes. Cardiovasc Ultrasound. 2014 Aug 12;12:33.
16. Altman M, Bergerot C, Aussoleil A, Davidsen ES, Sibellas F, Ovize M, et al. Assessment of left ventricular systolic function by deformation imaging derived from speckle tracking: a comparison between 2D and 3D echo modalities. Eur Heart J Cardiovasc Imaging. 2014 Mar;15(3):316-23. Epub 2013 Sep 18.
17. Delgado V, Tops LF, van Bommel RJ, van der Kley F, Marsan NA, Klautz RJ, et al. Strain analysis in patients with severe aortic stenosis and preserved left ventricular ejection fraction undergoing surgical valve replacement. Eur Heart J. 2009 Dec;30(24):3037-47.
18. Ye Z, Coutinho T, Pellikka PA, Villarraga HR, Borlaug BA, Kullo IJ. Associations of alterations in pulsatile arterial load with left ventricular longitudinal strain. Am J Hypertens. 2015 Nov;28(11):1325-31. Epub 2015 Apr 3.
19. Maréchaux S, Carpentier E, Six-Carpentier M, Asseman P, LeJemtel TH, Jude B, et al. Impact of valvuloarterial impedance on left ventricular longitudinal deformation in patients with aortic valve stenosis and preserved ejection fraction. Arch Cardiovasc Dis. 2010 Apr;103(4):227-35. Epub 2010 May 20.

20. Lang RM, Badano LP, Mor-Avi V, Afilalo J, Armstrong A, Ernande L, et al. Recommendations for cardiac chamber quantification by echocardiography in adults: an update from the American Society of Echocardiography and the European Association of Cardiovascular Imaging. J Am Soc Echocardiogr. 2015 Jan;28(1):1-39.e14.
21. Kaku K, Takeuchi M, Tsang W, Takigiku K, Yasukochi S, Patel AR, et al. Age-related normal range of left ventricular strain and torsion using three-dimensional speckle-tracking echocardiography. J Am Soc Echocardiogr. 2014 Jan;27(1):55-64. Epub 2013 Nov 13.
22. Kauer F, Geleijnse ML, van Dalen BM. Role of left ventricular twist mechanics in cardiomyopathies, dance of the helices. World J Cardiol. 2015 Aug 26;7(8):476-82.
23. Sallin EA. Fiber orientation and ejection fraction in the human left ventricle. Biophys J. 1969 Jul;9(7):954-64.
24. Notomi Y, Lysyansky P, Setser RM, Shiota T, Popovic ZB, Martin-Miklovic MG, et al. Measurement of ventricular torsion by two-dimensional ultrasound speckle tracking imaging. J Am Coll Cardiol. 2005 Jun 21;45(12):2034-41.
25. Helle-Valle T, Crosby J, Edvardsen T, Lyseggen E, Amundsen BH, Smith HJ, et al. New noninvasive method for assessment of left ventricular rotation: speckle tracking echocardiography. Circulation. 2005 Nov 15;112(20):3149-56.
26. van Dalen BM, Tzikas A, Soliman OI, Kauer F, Heuvelman HJ, Vletter WB, et al. Left ventricular twist and untwist in aortic stenosis. Int J Cardiol. 2011 May 5;148(3):319-24. Epub 2009 Dec 24.
27. Musa TA, Uddin A, Swoboda PP, Fairbairn TA, Dobson LE, Singh A, et al. Cardiovascular magnetic resonance evaluation of symptomatic severe aortic stenosis: association of circumferential myocardial strain and mortality. J Cardiovasc Magn Reson. 2017 Feb 8;19(1):13.
28. Abduch MC, Alencar AM, Mathias W Jr, Vieira ML. Cardiac mechanics evaluated by speckle tracking echocardiography. Arq Bras Cardiol. 2014 Apr;102(4):403-12.
29. Zito C, Salvia J, Cusma-Piccione M, Antonini-Canterin F, Lentini S, Oreto G, et al. Prognostic significance of valvuloarterial impedance and left ventricular longitudinal function in asymptomatic severe aortic stenosis involving three-cuspid valves. Am J Cardiol. 2011 Nov 15;108(10):1463-9. Epub 2011 Aug 25.
30. Kusunose K, Goodman A, Parikh R, Barr T, Agarwal S, Popovic ZB, et al. Incremental prognostic value of left ventricular global longitudinal strain in patients with aortic stenosis and preserved ejection fraction. Circ Cardiovasc Imaging. 2014 Nov;7(6):938-45. Epub 2014 Oct 15.
31. Yingchoncharoen T, Agarwal S, Popovic ZB, Marwick TH. Normal ranges of left ventricular strain: a meta-analysis. J Am Soc Echocardiogr. 2013 Feb;26(2):185-91. Epub 2012 Dec 3.
32. Magne J, Mohty D, Boulogne C, Deltreuil M, Cassat C, Echahidi N, et al. Prognostic impact of global left ventricular hemodynamic afterload in severe aortic stenosis with preserved ejection fraction. Int J Cardiol. 2015 Feb 1;180:158-64. Epub 2014 Nov 26.
33. Hachicha Z, Dumesnil JG, Pibarot P. Usefulness of the valvuloarterial impedance to predict adverse outcome in asymptomatic aortic stenosis. J Am Coll Cardiol. 2009 Sep 8;54(11):1003-11.

34. Pagel PS, Schroeder AR, De Vry DJ, Hudetz JA. Aortic valve replacement reduces valvuloarterial impedance but does not affect systemic arterial compliance in elderly men with degenerative calcific trileaflet aortic valve stenosis. J Cardiothorac Vasc Anesth. 2014 Dec;28(6):1540-4. Epub 2014 Sep 26.
35. Sato K, Seo Y, Ishizu T, Takeuchi M, Izumo M, Suzuki K, et al. Prognostic value of global longitudinal strain in paradoxical low-flow, low-gradient severe aortic stenosis with preserved ejection fraction. Circ J. 2014;78(11):2750-9. Epub 2014 Sep 30.
36. Kaku K, Takeuchi M, Tsang W, Takigiku K, Yasukochi S, Patel AR, et al. Age-related normal range of left ventricular strain and torsion using three-dimensional speckle-tracking echocardiography. J Am Soc Echocardiogr. 2014 Jan;27(1):55-64. Epub 2013 Nov 13.
37. Yodwut C, Weinert L, Klas B, Lang RM, Mor-Avi V. Effects of frame rate on three-dimensional speckle-tracking-based measurements of myocardial deformation. J Am Soc Echocardiogr. 2012 Sep;25(9):978-85. Epub 2012 Jul 4.

Tables

Table 1. Demographic and Clinical Characteristics of the Study Population[a]

Characteristics	Patients With AS (n=168)
Age, y	72±12
Women, No. (%)	70 (42)
Body surface area, m^2	1.95±0.26
Body mass index, kg/m^2	29±6
Heart rate, beats/min	67±12
Systolic blood pressure, mm Hg	129±18
Diastolic blood pressure, mm Hg	70±10
Cardiovascular risk factors (%)	
Diabetes mellitus	33
Systemic hypertension	80
Dyslipidemia	67
History of coronary artery disease	49
Current tobacco use	12
NYHA functional class	2.0±0.9
NT-proBNP, pg/mL	1,838±3,873

Abbreviations: AS, aortic valve stenosis; NT-proBNP, N-terminal fragment of the prohormone brain natriuretic peptide; NYHA, New York Heart Association.

[a] Data are expressed as mean±SD or as percentages unless otherwise indicated.

Table 2. Parameters in 2D and 3D Echocardiography for the Study (AS) and Normal Values From the Literature[a]

Parameter	2D (n=168)	Normal Values[b]	*P* Value	3D (n=168)[c]	*P* Value[d]
LVEDD, mm	48.2±5.9	44.3±4.8	<.001		
LVESD, mm	30.0±5.2	29.9±4.7	.72		
IVSd, mm	12±2	8±2	<.001		
LVPWd, mm	11±2	8.8±1.5	<.001		
LVEDV, mL	127±45	106±22	<.001	123±37	<.001
LVESV, mL	47±25	41±10	<.001	48±19	<.001
SV, mL	73.6±21.3	67±11	<.001	75±21	<.001
LVEF, %	63.4±6.1	63.9±4.9	.20	61±5	<.001
LV mass, g	220±75	150	<.001		
E velocity, m/s	1.0±0.4	0.09	<.001		
A velocity, m/s	1.0±0.4	0.076	<.001		
E/A ratio	0.94±0.36	1.18±0.4	<.001		
e'_{sep}	0.05±0.02	14.0±3.1	<.001		
E/e′ ratio, m	17.26±7.5	4.0±1.0	<.001		
Peak velocity, m/sec	4.4±0.5	NA			
Mean gradient, mm Hg	49±12	NA			
AVA, cm^2	0.89±0.16	NA			
AVA index, cm^2/m^2	0.46±0.07	NA			

Abbreviations: AS, aortic valve stenosis; AVA, aortic valve area; $e¢_{sep}$, early diastolic tissue Doppler velocity at the septal mitral annulus; E, peak velocity of early diastolic transmitral flow; E/A ratio, ratio of early and late diastolic waves of mitral inflow; E/e¢ ratio, ratio of the early wave of mitral inflow and early diastolic tissue Doppler velocity at the septal mitral annulus; IVSd, interventricular septum diameter; LV, left ventricular; LVEDD, left ventricular end-diastolic diameter; LVEDV, left ventricular end-diastolic volume; LVEF, left ventricular ejection fraction; LVESD, left ventricular end-systolic diameter; LVESV, left ventricular end-systolic volume; LVPWd, left ventricular posterior wall diameter; NA, not applicable; SV, stroke volume.

[a] Data are expressed as mean±SD unless otherwise indicated.

[b] Normal values are from guidelines of the American Society of Echocardiography (20).

[c] Not all data were available for 3D echocardiography.

[d] *P*□.01, 2D vs 3D.

[d] *P* value comparing 2D vs 3D values.

Table 3. Parameters of 2D– and 3D–Speckle-Tracking Strain in Study Patients (AS) and Normal Values From the Literature[a]

Parameter	2D (n=168)	Normal Values	*P* Value	3D (n=168)	*P* Value
GLS,%	–16.2±2.1	–21.5±2.0	<.001	–14.5±1.9	<.001
GRS,%	37.5±8.2	35.6±10.3	.02	41.6±9.8	<.001
GCS,%	–27.4±4.6	–30.6±2.6	<.001	–30.5±7.1	.60
Rot_{max}-A, °	10.7±4.0	12.79±4.3	<.001		
Rot_{max}-B, °	–7.8±2.2	–1.7±2.1	<.001		
$Twist_{max}$, °	18.5±4.7	12.7±4.8 (21)	<.001	13.7±7.0	.008
Torsion		1.75±0.66		1.6±0.8	.0004

Abbreviations: 2D, 2-dimensional; 3D, 3-dimensional; AS, aortic valve stenosis; GCS, global circumferential strain; GLS, global longitudinal strain; GRS, global radial strain; Rot_{max}-A, apical peak systolic rotation; Rot_{max}-B, basal peak systolic rotation; $Twist_{max}$, peak systolic twist.

[a] Data are expressed as mean±SD.

Table 4. Intraobserver and Interobserver Variability for 2D– and 3D–STE Measurements

	Intraobserver			Interobserver		
	Mean Difference±SD			Mean Difference±SD		
Measurement		ICC	*P* Value		ICC	*P* Value
3D–GLS, %	0.40±0.78	0.95	<.001	–0.08±1.46	0.84	<.001
3D–GRS, %	0.85±0.89	0.87	<.001	1.38±3.81	0.82	<.001
3D–GCS, %	0.25±3.72	0.90	<.001	0.67±3.48	0.89	<.001
3D–GPTS, %	–0.28±2.90	0.94	<.001	0.25±2.97	0.92	<.001
3D–Twist, °	–0.07±0.76	0.87	<.001	0.01±0.65	0.89	<.001
3D Torsion, °/cm	–0.10±0.33	0.88	<.001	–0.09±0.39	0.84	<.001
2D–GLS, %	–0.08±0.17	0.93	<.001	0.40±0.95	0.88	<.001
2D–GLSR, 1/s	0.04±0.08	0.88	<.001	–0.03±0.09	0.86	<.001
2D–GRS, %	–0.12±1.17	0.85	<.001	–0.15±4.70	0.86	<.001
2D–GRSR, 1/s	0.13±0.19	0.91	<.001	0.05±0.19	0.91	<.001
2D–GCS, %	–0.33±2.59	0.92	<.001	1.01±2.88	0.90	<.001
2D–GCSR,1/s	0.01±0.31	0.91	<.001	–0.13±0.32	0.87	<.001
2D–$Twist_{max}$, °	0.23±2.69	0.86	<.001	0.06±1.92	0.93	<.001

Abbreviations: 2D, 2-dimensional; 3D, 3-dimensional; GCS, global circumferential strain; GCSR, global circumferential strain rate; GLS, global longitudinal strain; GLSR, global longitudinal strain rate; GPTS, global principal tangential strain; GRS, global radial strain; GRSR, global radial strain rate; ICC, intraclass correlation coefficient; $Twist_{max}$, peak systolic twist.

Figures

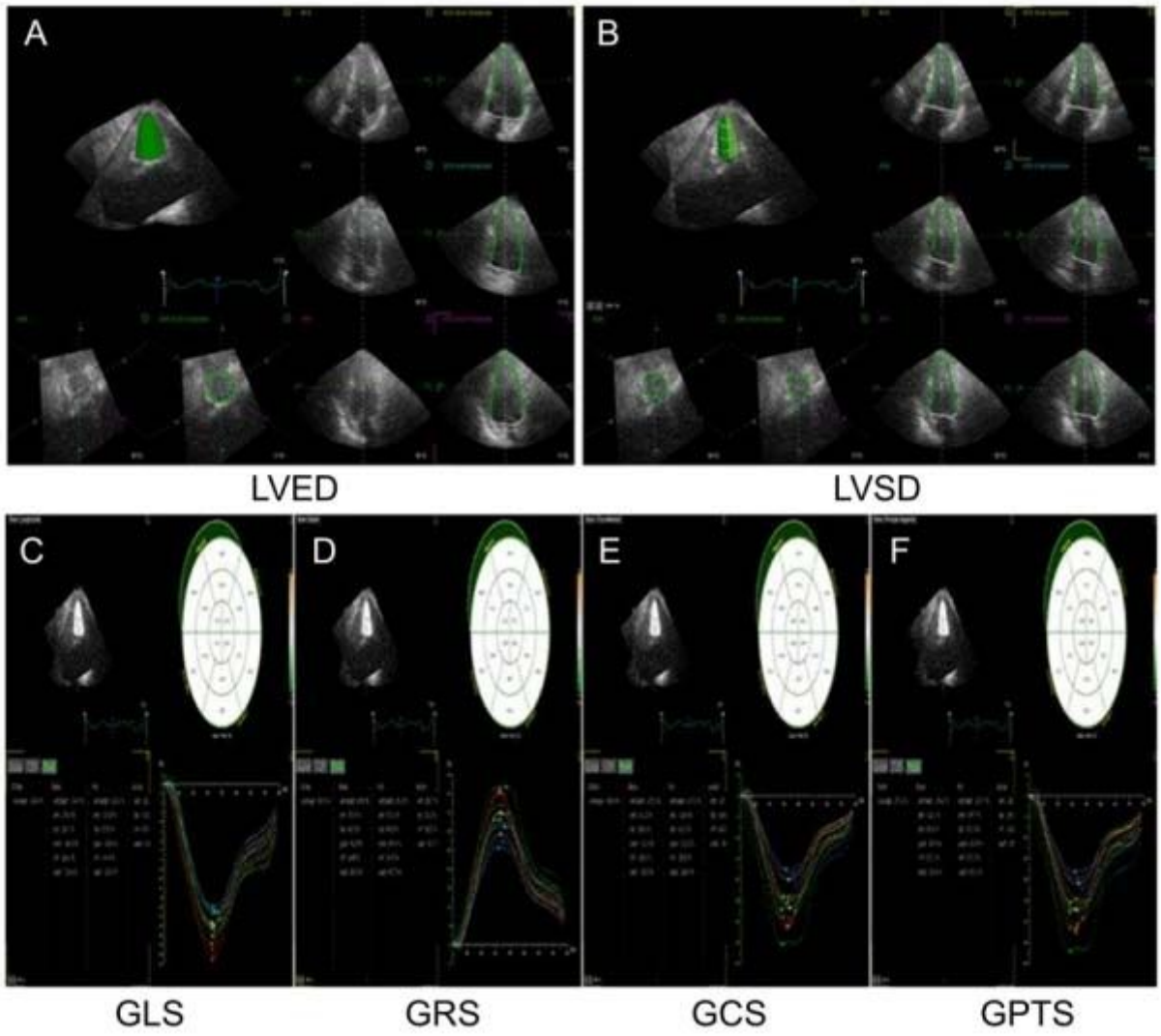

Figure 1

3-Dimensional (3D) Speckle Tracking With TomTec 4D Echo Software (TomTec Imaging Systems, Image Arena, Unterschleissheim, Germany). A and B, Standard 3 apical views and 1 short-axis view were automatically extracted from the 3D full-volume data sets. The 3D endocardial surface was automatically reconstructed at end-diastole (LVED) and end-systole (LVSD). C-F, The software anatomically provides longitudinal (GLS), radial (GRS), circumferential (GCS), and principal tangential strain (GPTS) time curves in 16 segments and, accordingly, peak global strain as well as averaged peak strain at 3 LV levels (basal, mid-ventricular, and apical). LV indicates left ventricular.

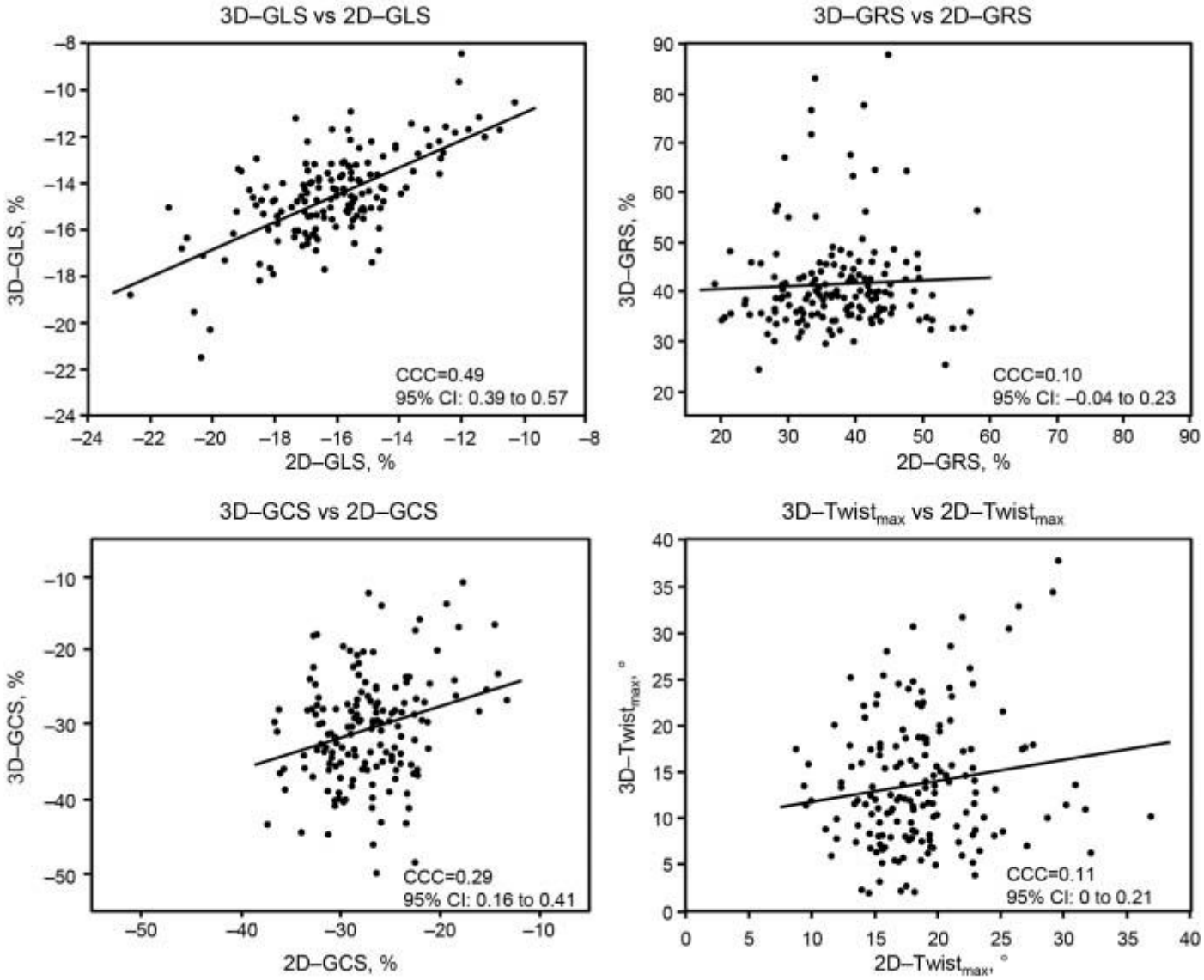

Figure 2

Agreement Between Parameters of Strain in 2-dimensional (2D) and 3-dimension (3D). 2D–GCS indicates global circumferential strain measured by 2D echocardiography; 2D–GLS, global longitudinal strain measured by 2D echocardiography; 2D–GRS, global radial strain measured by 2D echocardiography; 3D–GCS, global circumferential strain measured by 3D echocardiography; 3D–GLS, global longitudinal strain measured by 3D echocardiography; 3D–GRS, global radial strain measured by 3D echocardiography; 2D–Twistmax, LV twist measured by 2D echocardiography; 3D–Twistmax, LV Twistmax measured by 3D echocardiography. CCC indicates concordance correlation coefficient; LV, left ventricular; Twistmax, peak systolic twist.

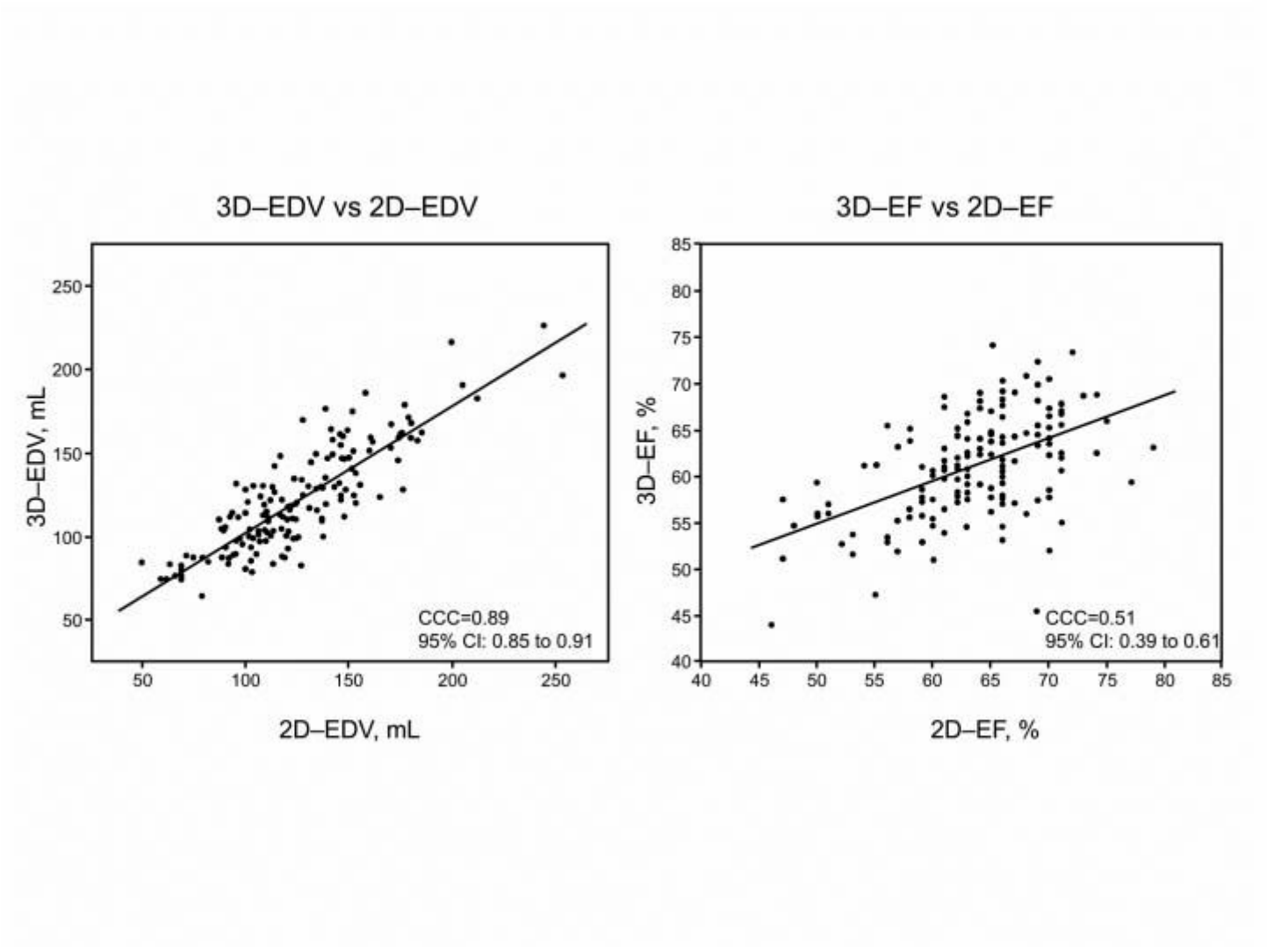

Figure 3

Agreement Between Parameters of Conventional Echocardiography in 2-dimensional (2D) and 3-dimensional (3D). 2D–EDV indicates left ventricular end-diastolic volume measured by 2D echocardiography; 2D–EF, left ventricular ejection fraction measured by 2D echocardiography; 3D–EDV indicates left ventricular end-diastolic volume measured by 3D echocardiography; 3D–EF, left ventricular ejection fraction measured by 3D echocardiography. CCC indicates concordance correlation coefficient.